

STUDY OF MOLECULAR STRUCTURE, VIBRATIONAL ELECTRONIC SPECTRA AND NLO PROPERTIES OF (2E)-1-(4-bromophenyl)-3-(4-nitrophenyl) Prop-2-en-1-one BY DFT

Dr. Raksha Gupta

Associate Professor, Department of Chemistry,
A.S. (P.G.) College, Mawana, Meerut

Abstract—The molecular structure of (2E)-1-(4-bromophenyl)-3-(4-nitrophenyl)prop-2-en-1-one with $C_{15}H_{10}BrN_1O_3$ empirical formula was simulated using B3LYP levels of density functional theory. After geometrical optimization on the ground state of the chalcone studied a detailed vibrational spectral analysis was carried out and the assignments of the observed bands have been proposed on the basis of values reported in literature. UV-Visible spectral study was done by time-dependent TD-DFT approach B3LYP level and Electronic transitions were calculated, and the important contributions from the molecular orbitals to the electronic transitions were investigated. HOMO–LUMO analysis has been done in order to determine the way the molecule interacts with other species. HOMO and LUMO energies were calculated. On the basis of vibrational analysis, other molecular properties such as ionization energy, electron affinity, chemical potential, global hardness and electrophilicity were calculated by time-dependent TD-DFT approach. The electrical properties determined were the dipole moment (μ), mean polarizability (α), anisotropy of the polarizability ($\Delta\alpha$), first and second order hyperpolarizabilities (β and γ) in terms of x, y, z components from Gaussian 09 output.

KEYWORDS: DFT, HOMO, LUMO, CHALCONE, VIBRATIONAL SPECTRA, ELECTRONIC TRANSITIONS

INTRODUCTION

Chalcone is a compound consists of two aromatic rings linked by an unsaturated α, β -ketone, with various substituent's on the two aromatic rings. General Structure of Chalcones is shown in Figure-1

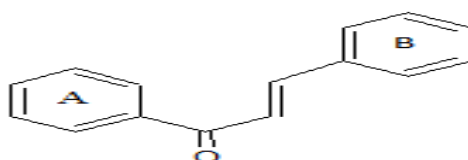


Figure-1: General Structure of Chalcones

Chalcone could be easily found in most of the plants naturally and is an intermediate precursor of flavonoids and is of flavonoids [1]. Due to the extended conjugation, the complete delocalisation of p electrons on both the benzene rings makes it good for wide range of applications in the fields of biology and biochemistry[2,3] such as antitumor [4,5], anti-inflammatory[6–8], and antimalarial [9] agents. In modern years, chalcones have been used in the field of material science as optical limiting [10], electrochemical sensing [11] and Langmuir film [12]. Appreciation of these findings motivated us to carry out computational study of chalcones.

MATERIALS AND METHODS

Theoretical Calculation: The entire calculation was performed at DFT levels on a personal laptop using Gaussian(R) 09 program [13] program package, invoking gradient geometry optimization [13,14]. In the present study, the DFT/B3LYP/6-31G (d) basis set level was used to calculate the optimized parameters and vibrational wave numbers of the title molecule. The vibrational frequency assignments were made with a high degree of accuracy.

RESULTS AND DISCUSSIONS

Geometrical analysis: The first task for the computational work is to determine the optimized geometries of the studied chalcone molecule. The molecular structure along with numbering of atoms of (2*E*)-1-(4-bromophenyl)-3-(4-nitrophenyl)prop-2-en-1-one is shown in Fig. 2. The geometrical parameters of chalcone molecule studied are calculated using B3LYP with 6-31G (d) level of theory. In this study title chalcone molecule consist of two phenyl and a prop-2-en-1-one moieties. The optimized bond lengths, bond angles and dihedral angles of the studied are listed in Table-1 and is in accordance with atom numbering scheme as shown in Figure.2.

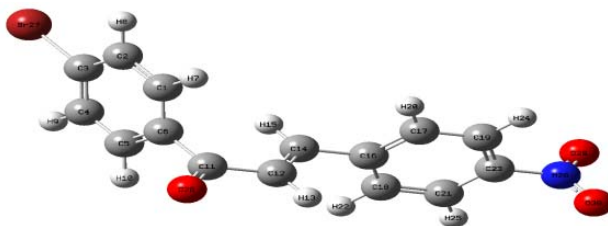


FIGURE-2: Optimised geometry of (2*E*)-1-(4-bromophenyl)-3-(4-nitrophenyl)prop-2-en-1-one

TABLE-1: OPTEMISED GEOMETERICAL PARAMETERS OF (2*E*)-1-(4-bromophenyl)-3-(4-nitrophenyl)prop-2-en-1-one at B3LYP/6-31G (d): bond length (Å), bond angle (°), dihedral angles (°)

S. No.	Atoms of molecule	Bond length (Å)	Angle between atoms	Bond angle (°)	Dihedral angle between atoms	Dihedral angle (°)
1	R(1,2)	1.3903	A(2,1,6)	120.9115	D(6,1,2,3)	1.305
3	R(1,6)	1.404	A(2,1,7)	120.4759	D(6,1,2,8)	-179.0696
3	R(1,7)	1.0851	A(6,1,7)	118.6126	D(7,1,2,3)	-178.6699
4	R(2,3)	1.3964	A(1,2,3)	119.0378	D(7,1,2,8)	0.9554
5	R(2,8)	1.0845	A(1,2,8)	120.8244	D(2,1,6,5)	-1.7919
6	R(3,4)	1.3935	A(3,2,8)	120.1367	D(2,1,6,11)	-178.2255
7	R(3,27)	1.9079	A(2,3,4)	121.2643	D(7,1,6,5)	178.1835
8	R(4,5)	1.3946	A(2,3,27)	119.3584	D(7,1,6,11)	1.7499
9	R(4,9)	1.0844	A(4,3,27)	119.376	D(1,2,3,4)	0.115
10	R(5,6)	1.4029	A(3,4,5)	119.1164	D(1,2,3,27)	179.6952
11	R(5,10)	1.0851	A(3,4,9)	120.1977	D(8,2,3,4)	-179.513
12	R(6,11)	1.4993	A(5,4,9)	120.6848	D(8,2,3,27)	0.0672
13	R(11,12)	1.4867	A(4,5,6)	120.7284	D(2,3,4,5)	-1.0104
14	R(11,26)	1.2272	A(4,5,10)	119.0823	D(2,3,4,9)	178.6181
15	R(12,13)	1.0872	A(6,5,10)	120.1601	D(27,3,4,5)	179.4095
16	R(12,14)	1.3479	A(1,6,5)	118.9164	D(27,3,4,9)	-0.962
17	R(14,15)	1.088	A(1,6,11)	117.6768	D(3,4,5,6)	0.5019
18	R(14,16)	1.4667	A(5,6,11)	123.3038	D(3,4,5,10)	178.538
19	R(16,17)	1.4082	A(6,11,12)	121.4664	D(9,4,5,6)	-179.1247
20	R(16,18)	1.4098	A(6,11,26)	120.1965	D(9,4,5,10)	-1.0886
21	R(17,19)	1.3901	A(12,11,26)	118.328	D(4,5,6,1)	0.8733
22	R(17,20)	1.0866	A(11,12,13)	112.6068	D(4,5,6,11)	177.0941
23	R(18,21)	1.3876	A(11,12,14)	125.5042	D(10,5,6,1)	-177.1417
24	R(18,22)	1.0849	A(13,12,14)	121.348	D(10,5,6,11)	-0.9209
25	R(19,23)	1.3924	A(12,14,15)	118.4037	D(1,6,11,12)	-153.1197
26	R(19,24)	1.0829	A(12,14,16)	126.887	D(1,6,11,26)	25.7623
27	R(21,23)	1.3957	A(15,14,16)	114.6894	D(5,6,11,12)	30.6156
28	R(21,25)	1.083	A(14,16,17)	118.4501	D(5,6,11,26)	150.5023
29	R(23,28)	1.4706	A(14,16,18)	123.2403	D(6,11,12,13)	-159.6076
30	R(28,29)	1.2307	A(17,16,18)	118.3089	D(6,11,12,14)	28.7815
31	R(28,30)	1.2308	A(16,17,19)	121.4049	D(26,11,12,13)	21.4901
32			A(16,17,20)	119.2804	D(26,11,12,14)	-150.1208
33			A(19,17,20)	119.3145	D(11,12,14,15)	-4.7208
34			A(16,18,21)	121.0001	D(11,12,14,16)	173.5631
35			A(16,18,22)	120.1182	D(13,12,14,15)	-175.647

36			A(21,18,22)	118.8815	D(13,12,14,16)	2.6368
37			A(17,19,23)	118.5202	D(12,14,16,17)	-176.5594
38			A(17,19,24)	121.8194	D(12,14,16,18)	3.7308
39			A(23,19,24)	119.6603	D(15,14,16,17)	1.7792
40			A(18,21,23)	118.9259	D(15,14,16,18)	-177.9306
41			A(18,21,25)	121.6104	D(14,16,17,19)	-179.8595
42			A(23,21,25)	119.4637	D(14,16,17,20)	0.2952
43			A(19,23,21)	121.8397	D(18,16,17,19)	-0.1352
44			A(19,23,28)	119.0864	D(18,16,17,20)	-179.9805
45			A(21,23,28)	119.0738	D(14,16,18,21)	179.8133
46			A(23,28,29)	117.6044	D(14,16,18,22)	-0.0729
47			A(23,28,30)	117.6135	D(17,16,18,21)	0.1031
48			A(29,28,30)	124.7821	D(17,16,18,22)	-179.7831
49					D(16,17,19,23)	0.0834
50					D(16,17,19,24)	-179.9344
51					D(20,17,19,23)	179.9287
52					D(20,17,19,24)	-0.0892
53					D(16,18,21,23)	-0.0212
54					D(16,18,21,25)	-179.9814
55					D(22,18,21,23)	179.8664
56					D(22,18,21,25)	-0.0938
57					D(17,19,23,21)	0.0027
58					D(17,19,23,28)	179.9309
59					D(24,19,23,21)	-179.9798
60					D(24,19,23,28)	-0.0516
61					D(18,21,23,19)	-0.0334
62					D(18,21,23,28)	-179.9616
63					D(25,21,23,19)	179.9277
64					D(25,21,23,28)	-0.0006
65					D(19,23,28,29)	-179.9955
66					D(19,23,28,30)	-0.0091
67					D(21,23,28,29)	-0.0652
68					D(21,23,28,30)	179.9211

Vibrational Assignments

The fundamental vibrations of a non-linear molecule which contains N atoms is equal to $(3N-6)$, apart from three translational and three rotational degrees of freedom [15, 16]. The studied chalcone molecule belongs to Cs point group symmetry and has 30 atoms; hence 84 normal modes of vibrations are possible. All vibrations are active in both IR and Raman absorption

The vibrational assignments were made by the values reported in literature [15]. In the aromatic compounds, the C-H stretching vibrations normally occur at $3100-3000\text{ cm}^{-1}$. In this region, the bands are not affected appreciably by the nature of substituents [15]. The C-H stretching vibration was observed at 3078 cm^{-1} [17], and these peaks were calculated at 3074 and 3070 cm^{-1} (mode 77 and 76 respectively) for B3LYP level. The aromatic ring in-plane C-H bending vibrations are usually weak and observed in the region $1300-1000\text{ cm}^{-1}$, while the out-of-plane ones lie in the region $900-650\text{ cm}^{-1}$ [18]. In our calculations in-plane C-H bending vibrations are assigned at the wave number regions of $1291-1045\text{ cm}^{-1}$ (mode 60 to 48) and 680 cm^{-1} (mode 30). The peak at 807 cm^{-1} (mode 34) for B3LYP is assigned as the out of plane C-H bending vibration. The IR spectrum shows the characteristic absorption bands at 1650 cm^{-1} due to C=O group of α , β -unsaturated carbonyl compound [17]. This characteristic C=O band is calculated at 1600 cm^{-1} (mode 72) for B3LYP level. The NO₂ stretching vibrations which are another characteristic vibration mode were observed at 1519 cm^{-1} for asymmetric stretch and 1312 cm^{-1} for symmetric stretch [17]. It is well known that asymmetric vibrations appear at higher frequencies than symmetric ones for nitro group vibrations. These vibrations were assigned at 1548 cm^{-1} (mode 68) and 1340 cm^{-1} (mode 63) for B3LYP level. The ring C=C stretching vibrations usually occur in the region $1625-1280\text{ cm}^{-1}$ [19]. For aromatic six-membered rings such as benzene, there are two or three bands in this region due to skeletal vibrations, the strongest one at about 1500 cm^{-1} [20]. The peak observed at 1569 cm^{-1} was assigned the C=C stretching vibration [17]. This vibration mode was calculated at the ranges of $1589-1192\text{ cm}^{-1}$ (mode 71 to 55) for B3LYP level. The calculated peaks at 986 cm^{-1} (mode 45) and 825 cm^{-1} (mode 36) for B3LYP level were attributed to in plane C-C bending vibrations. The out of plane C-C vibration was calculated at 747 and 736 cm^{-1} (mode 33 and 32). The frequency were calculated using DFT/B3LYP/6-31G (d) basis set are listed in Table 2 and presented in figure 3 and 4

TABLE-2: Calculated Frequencies of (2E)-1-(4-bromophenyl)-3-(4-nitrophenyl) prop-2-en-1-one

MODE	FREQUENCY (cm ⁻¹)		INFRARED	RAMAN ACTIVITY	DEPOLR-P	DEPOLAR-U	Assignments
	Unscaled	Scaled					
1	18.26	17.54	0.0250	7.2193	0.7499	0.8571	
2	24.98	24.00	0.3576	4.6870	0.7030	0.8256	
3	35.32	33.94	1.8251	4.1855	0.7368	0.8485	
4	64.39	61.87	0.0455	0.2374	0.7192	0.8367	
5	71.64	68.83	3.6701	4.1768	0.7180	0.8359	
6	84.68	81.36	1.1074	1.3647	0.6051	0.7540	
7	104.01	99.93	2.8709	1.1321	0.6754	0.8063	
8	137.73	132.33	4.8589	3.6245	0.6296	0.7727	
9	158.48	152.27	2.7658	1.1978	0.6667	0.8000	
10	177.13	170.19	1.8287	3.6940	0.5807	0.7347	
11	235.11	225.89	0.3828	3.0856	0.6632	0.7975	
12	247.51	237.80	1.3306	3.5019	0.7409	0.8512	
13	264.37	254.01	3.5849	1.7964	0.4718	0.6411	
14	283.69	272.57	1.0835	1.3086	0.6452	0.7843	
15	333.19	320.13	3.4006	3.7303	0.6169	0.7631	
16	352.93	339.10	2.4792	1.4906	0.3028	0.4648	
17	419.48	403.04	0.3513	0.1224	0.4800	0.6486	
18	425.61	408.92	3.2220	1.6009	0.4076	0.5791	
19	428.79	411.98	8.7781	2.1998	0.4219	0.5934	
20	454.53	436.71	15.0496	1.3386	0.4368	0.6080	
21	484.83	465.82	4.4725	0.8462	0.3869	0.5580	
22	499.19	479.62	3.1132	1.5211	0.5044	0.6706	
23	536.76	515.72	1.3077	2.6273	0.7499	0.8571	
24	567.03	544.80	7.1646	7.7486	0.1944	0.3256	
25	639.64	614.56	12.2622	8.3070	0.5276	0.6907	C-Br stretching
26	641.64	616.49	1.3371	5.3818	0.7294	0.8436	
27	648.88	623.44	7.8035	6.8798	0.5088	0.6744	
28	672.92	646.54	6.0558	2.2519	0.5921	0.7438	
29	691.90	664.78	7.5320	14.4244	0.1135	0.2038	
30	708.29	680.52	11.3850	0.6343	0.4468	0.6176	In-plane C-H bending vibration
31	748.45	719.11	8.1982	9.5731	0.2203	0.3611	
32	766.95	736.89	17.1781	5.5585	0.1470	0.2563	C-C Out-of-plane bending vibration
33	777.49	747.01	46.8139	8.3277	0.7493	0.8567	Out-of-plane bending vibration
34	840.26	807.32	22.6013	22.1049	0.3151	0.4793	Out-of-plane bending vibration of C-H
35	848.44	815.18	3.1492	5.3339	0.5727	0.7283	
36	859.23	825.55	55.0375	19.5331	0.2712	0.4267	C-C In-plane bending vibration
37	859.60	825.91	12.7890	4.8876	0.7218	0.8385	
38	873.44	839.20	19.9595	10.6197	0.1042	0.1887	In-plane C-H bending vibration
39	886.43	851.68	31.4429	7.7609	0.2588	0.4112	
40	913.27	877.47	9.9208	20.0804	0.4941	0.6614	
41	982.97	944.44	0.1598	0.5956	0.5340	0.6962	
42	986.53	947.86	4.7226	1.9562	0.6648	0.7986	
43	992.25	953.35	3.7459	5.8414	0.5638	0.7211	
44	995.91	956.87	0.9858	2.2693	0.4359	0.6072	
45	1026.78	986.53	72.8177	0.7215	0.4452	0.6161	C-C In-plane bending vibration
46	1031.66	991.22	35.9767	43.5307	0.2701	0.4254	

47	1032.83	992.34	3.8371	4.6051	0.5441	0.7048	
48	1088.32	1045.66	17.8314	142.9800	0.1710	0.2920	In-plane C-H bending vibration
49	1101.13	1057.97	100.1140	22.3961	0.3316	0.4981	In-plane C-H bending vibration
50	1133.18	1088.76	60.2399	265.4497	0.2604	0.4132	In-plane C-H bending vibration
51	1140.04	1095.35	7.4931	1.4901	0.6254	0.7696	In-plane C-H bending vibration
52	1140.15	1095.46	3.4526	0.9979	0.5426	0.7035	
53	1211.60	1164.11	40.9305	9.5249	0.5669	0.7236	
54	1216.79	1169.09	0.6250	112.0247	0.2469	0.3960	
55	1240.74	1192.10	30.5939	246.6901	0.3716	0.5418	In-plane C-H bending vibration
56	1287.00	1236.55	190.2956	409.2981	0.2159	0.3551	Aromatic six membered ring skeletal vibration
57	1314.62	1263.08	251.6677	183.8896	0.4522	0.6228	Aromatic six membered ring skeletal vibration
58	1334.00	1281.71	23.3148	1.9141	0.2742	0.4304	In-plane C-H bending vibration
59	1335.85	1283.48	8.6586	3.4317	0.2306	0.3748	In-plane C-H bending vibration
60	1344.65	1291.94	34.7463	5.9568	0.3172	0.4817	In-plane C-H bending vibration
61	1362.58	1309.17	4.4209	48.2609	0.2562	0.4079	Aromatic six membered ring skeletal vibration
62	1385.74	1331.42	22.1449	16.2914	0.6499	0.7878	Aromatic six membered ring skeletal vibration
63	1395.29	1340.59	457.4470	837.8734	0.2972	0.4582	Symmetric NO ₂ stretching vibration
64	1438.57	1382.18	23.5531	10.6708	0.2195	0.3600	Aromatic six membered ring skeletal vibration
65	1458.23	1401.07	21.6860	64.1772	0.3694	0.5396	Aromatic six membered ring skeletal vibration
66	1530.59	1470.59	11.3127	5.0939	0.3232	0.4885	Aromatic six membered ring skeletal vibration
67	1541.68	1481.25	6.8208	20.2189	0.2995	0.4610	Aromatic six membered ring skeletal vibration
68	1612.08	1548.89	88.1757	54.5465	0.3502	0.5188	Asymmetric NO ₂ stretching vibration
69	1615.02	1551.72	21.7408	13.9114	0.1851	0.3123	Aromatic six membered ring skeletal vibration
70	1642.02	1577.65	120.1142	363.5208	0.3921	0.5633	Aromatic six membered ring skeletal vibration
71	1653.97	1589.13	16.8076	2350.7992	0.3636	0.5333	Aromatic six membered ring skeletal vibration
72	1665.42	1600.14	112.9861	149.1596	0.3386	0.5060	C=O vibration of α,β -unsaturated carbonyl group

73	1690.79	1624.51	39.2217	1652.3325	0.3288	0.4949	Aromatic six membered ring skeletal vibration
74	1730.60	1662.76	222.2567	556.9831	0.1974	0.3297	Aromatic six membered ring skeletal vibration
75	3180.02	3055.36	5.9680	48.2342	0.2838	0.4421	Aromatic six membered ring skeletal vibration
76	3195.45	3070.18	7.2491	52.3114	0.4389	0.6101	Aromatic six membered ring skeletal vibration
77	3199.78	3074.35	11.1474	46.3252	0.3953	0.5666	Aromatic six membered ring skeletal vibration
78	3213.19	3087.24	3.1509	44.2085	0.5094	0.6749	
79	3219.47	3093.27	0.1818	51.8316	0.7183	0.8361	
80	3219.74	3093.52	4.6958	42.1573	0.4286	0.6000	
81	3229.32	3102.73	3.4001	46.6307	0.1533	0.2659	
82	3232.34	3105.63	2.0514	193.1281	0.1674	0.2868	
83	3254.11	3126.55	0.8104	90.0575	0.2684	0.4232	
84	3254.79	3127.20	0.9773	89.7059	0.2258	0.3684	

HOMO- LUMO and Reactive descriptors

The Eigen values of HOMO (π - donor) and LUMO (π - acceptor) and their energy gap reflect the chemical activity of the molecules. Recently, the energy gap between HOMO and LUMO has been used to prove the microscopic NLO activity from intra-molecular charge transfer (ICT). Also, energies of HOMO and LUMO are used for the determination of global reactivity descriptors. It is important that Ionization potential (I), Electron affinity (A), Electrophilicity (ω), Chemical potential (μ), Electro negativity (χ), Hardness (η) and Softness (S) be put into a MO framework. We focus on the HOMO and LUMO energies in order to determine the interesting molecular/atomic properties and chemical quantities. In simple molecular orbital theory approaches, the HOMO energy is related to the ionization potential (I) and the LUMO energy has been used to estimate the electron affinity (A) respectively by the following relations[28]:

$$I = -EHOMO \text{ and}$$

$$A = -ELUMO$$

The chemical potential of the molecule is $(\phi) = -(I + A)/2$.

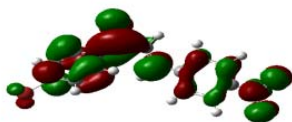
The absolute hardness of the molecule is $(\eta) = (I - A)/2$.

The softness is the inverse of the hardness $(S) = 1/\eta$.

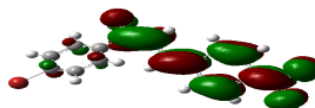
The electro negativity of the molecule is $(\chi) = (I + A)/2$.

The electrophilicity index of the molecule is $(\omega) = \phi^2/2\eta$.

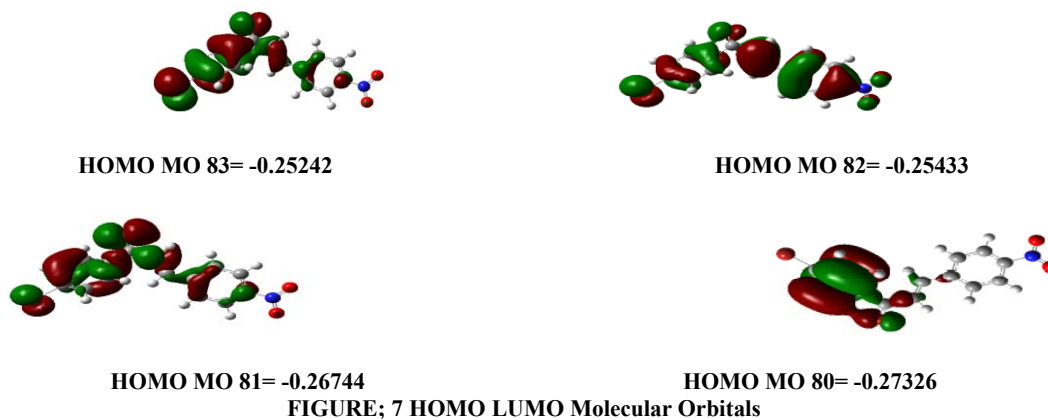
This value assesses energy decreasing due to maximal electron flow between donor (HOMO) and acceptor (LUMO) shown in figure 7. The calculated values of the global reactivity descriptors for the title molecule are collected in table 5 and Energy gap (ΔE) in HOMO LUMO is tabulated in table-4. . In terms of chemical hardness, if a molecule has a large HOMO–LUMO gap, it is hard. Conversely, if the HOMO–LUMO gap is small, it is soft. One can also relate molecular stability to hardness, which means that the molecule with smaller HOMO–LUMO gap is more reactive.



LUMOMO 85 = -0.07111



LUMO MO 84= -0.10854



Electrostatic potential (ESP)

Molecular electrostatic potential (MEP) or Electrostatic potential (ESP) maps are very useful three dimensional diagrams which are used to visualize the charge distributions and charge related properties of molecules. Also, MEP or ESP picture has been used to predict the reactive sites for electrophilic and nucleophilic attack, and in studies of biological recognition and hydrogen bonding interactions [24-25]. The ESP of the studied compound calculated using B3LYP method with 6-31G (d) basis set is shown in Fig. 8a, 8b, and 8c. It can be seen from the ESP figure; negative regions (red) are mainly localized over the carbonyl oxygen atom and bromine atom while the positive regions (blue) are distributed over the H-atoms

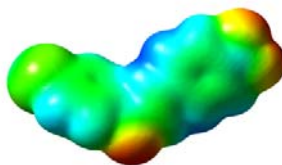


Figure 8c ELECTRON DENSITY TOTAL SCF DENSITY (Isovalue=0.0004,(mapped with ESP)

NLO PROPERTIES

NLO is the important role of current research because it provides the key functions of frequency shifting, optical logic, optical modulation, optical switching and optical memory for the technologies in areas such as telecommunications, signal processing and optical interconnection [21, 22].

The density functional theory has been used to calculate the dipole moment (μ), mean polarizability (α), anisotropy of the polarizability ($\Delta\alpha$), first and second order hyperpolarizabilities (β and γ) in terms of x, y, z components from Gaussian 09 output.

For a molecule the μ , α , $\Delta\alpha$, β and γ are defined as follows [23]:

$$\mu = (\mu_x + \mu_y + \mu_z)^{1/2}$$

$$\langle \alpha \rangle = \frac{1}{3}(\alpha_{xx} + \alpha_{yy} + \alpha_{zz})$$

$$\Delta\alpha = \frac{1}{\sqrt{2}}[(\alpha_{xx} - \alpha_{yy})^2 + (\alpha_{yy} - \alpha_{zz})^2 + (\alpha_{zz} - \alpha_{xx})^2 + 6(\alpha_{xy}^2 + \alpha_{yz}^2 + \alpha_{zx}^2)]^{1/2}$$

$$\beta = [(\beta_{xxx} + \beta_{xyy} + \beta_{xzz})^2 + (\beta_{yyy} + \beta_{yzz} + \beta_{yxx})^2 + (\beta_{zzz} + \beta_{zxx} + \beta_{zyy})^2]^{1/2}$$

$$\gamma = \frac{1}{5}[\gamma_{xxxx} + \gamma_{yyyy} + \gamma_{zzzz} + 2(\gamma_{xxyy} + \gamma_{xxzz} + \gamma_{yyzz})]$$

TABLE-6: Calculated dipole moment (μ , in Debye), mean polarizability (α_0 , in a.u.), anisotropy of polarizability ($\Delta\alpha$, in a.u.) and first hyper polarizability (β , in a.u.) of (2*E*)-1-(4-bromophenyl)-3-(4-nitrophenyl)prop-2-en-1-one

Dipole moment (Debye):	
μ_x	-2.6546
μ_y	-0.7903;
μ_z	0.1349
Total μ	2.7730
Polarizability in a.u.	
α_{xx}	-166.2574
α_{yy}	-134.5106
α_{zz}	-123.2827
α_{xy}	11.6527
α_{xz}	2.7649
α_{yz}	0.2824
α	-141.3502
$\Delta\alpha$	43.8347
$\Delta\alpha$	43.8347×10^{-30} esu
First order hyper polarizability in a.u.	
β_{xxx}	-496.8919
β_{yyy}	-94.0155
β_{zzz}	1.2173
β_{xyy}	-40.2855
β_{xxy}	81.6859
β_{xxz}	-15.7793
β_{xzz}	-42.0926
β_{yzz}	-15.1151
β_{yyz}	6.1362
β_{xyz}	14.0173
β	579.98098
β	$579.98098 \times 10^{-30}$ esu
Second order hyper polarizability in a.u.	
γ_{xxxx}	-16800.9538
γ_{yyyy}	-1973.3926
γ_{zzzz}	-282.8921
γ_{xxxxy}	769.9938
γ_{xxxz}	45.8793
γ_{yyyx}	321.8364
γ_{yyyz}	14.5233
γ_{zzzx}	-1.9342
γ_{zzzy}	-7.5568
γ_{xxyy}	-2645.3294
γ_{xxzz}	-2296.8207
γ_{yyzz}	-323.9044
γ_{xxyz}	-52.1833
γ_{yyxz}	29.3319
γ_{zzxy}	48.5874
γ	-4551.72422
γ	$-4551.72422 \times 10^{-30}$ esu

References

- [1] G. Achanta, A. Modzelewska, L. Feng, S. R. Khan, and P.Huang, "A boronic-chalcone derivative exhibits potent anticancer Activity through inhibition of the proteasome," *Molecular Pharmacology*, vol. 70, no. 1, pp. 426–433, 2006.
- [2] S.N.A. Bukhari, M. Jasamai, I. Jantan, and W.Ahmad, "Reviews of methods and various catalysts used for chalcone synthesis," *Mini-Reviews in Organic Chemistry*, vol. 10, pp. 73–83, 2013.
- [3] S. N. A. Bukhari, M. Jasamai, and I. Jantan, "Synthesis and Biological evaluation of chalcone derivatives (mini review)," *Mini Review of Medicinal Chemistry*, vol. 12, no. 13, pp. 1384–1403, 2012.
- [4] G. Saydam, H. H. Aydin, F. Sahin et al., "Cytotoxic and Inhibitory effects of 4, 4'-dihydroxy chalcone (RVC-588) on Proliferation of human leukemic HL-60 cells," *Leukemia Research*, vol. 27, no. 1, pp. 57–64, 2003.

- [5] L. Mishra, R. Sinha, H. Itokawa et al., "Anti-HIV and cytotoxic activities of Ru(II)/Ru(III) polypyridyl complexes containing 2,6-(2-benzimidazolyl)-pyridine/chalcone as co-ligand," *Bioorganic and Medicinal Chemistry*, vol. 9, no. 7, pp. 1667–1671, 2001.
- [6] H.-H. Ko, L.-T. Tsao, K.-L. Yu, C.-T. Liu, J.-P. Wang, and C.-N. Lin, "Structure-activity relationship studies on chalcone derivatives: the potent inhibition of chemical mediators release," *Bioorganic and Medicinal Chemistry*, vol. 11, no. 1, pp. 105–111, 2003.
- [7] P. Tuchinda, V. Reutrakul, P. Claeson et al., "Anti-inflammatory cyclohexenyl chalcone derivatives in *Boesenbergia pandurata*," *Phytochemistry*, vol. 59, no. 2, pp. 169–173, 2002.
- [8] S. N. A. Bukhari, I. Jantan, and M. Jasamai, "Anti-inflammatory trends of 1, 3-diphenyl-2-propen-1-one derivatives," *Mini-Reviews in Medicinal Chemistry*, vol. 13, pp. 87–94, 2013.
- [9] J. N. Domínguez, C. León, J. Rodrigues, N. G. De Domínguez, J. Gut, and P. J. Rosenthal, "Synthesis and evaluation of new antimalarial phenylurenyl chalcone derivatives," *Journal of Medicinal Chemistry*, vol. 48, no. 10, pp. 3654–3658, 2005.
- [10] S. Shettigar, K. Chandrasekharan, G. Umesh, B. K. Sarojini, Studies on nonlinear optical parameters of bis-chalcone derivatives doped polymer, *Polymer*, **2006**, 47, 3565.
- [11] A. Delavaux, B. Nicot, J. Maynadie, D. Lavabre, Ca²⁺ vs. Ba²⁺ electrochemical detection by two disubstituted ferrocenyl chalcone chemosensors. Study of the ligand–metal interactions in CH₃CN, *J. Organometallic Chem.*, **2007**, 692, 874.
- [12] E. I. Gasull, S. E. Blanco, F. H. Ferretti, A theoretical and experimental study of adsorption from dilute cyclohexane solutions of non-electrolytes: 4-X-chalcones on silica gel, *J. Mol. Struct. (Theochem)*, **2002**, 579, 121.
- [13] Gaussian 09, Revision D.01, M. J. Frisch, G. W. Trucks, H. B. Schlegel, G. E. Scuseria, M. A. Robb, J. R. Cheeseman, G. Scalmani, V. Barone, B. Mennucci, G. A. Petersson, H. Nakatsuji, M. Caricato, X. Li, H. P. Hratchian, A. F. Izmaylov, J. Bloino, G. Zheng, J. L. Sonnenberg, M. Hada, M. Ehara, K. Toyota, R. Fukuda, J. Hasegawa, M. Ishida, T. Nakajima, Y. Honda, O. Kitao, H. Nakai, T. Vreven, J. A. Montgomery, Jr., J. E. Peralta, F. Ogliaro, M. Bearpark, J. J. Heyd, E. Brothers, K. N. Kudin, V. N. Staroverov, T. Keith, R. Kobayashi, J. Normand, K. Raghavachari, A. Rendell, J. C. Burant, S. S. Iyengar, J. Tomasi, M. Cossi, N. Rega, J. M. Millam, M. Klene, J. E. Knox, J. B. Cross, V. Bakken, C. Adamo, J. Jaramillo, R. Gomperts, R. E. Stratmann, O. Yazyev, A. J. Austin, R. Cammi, C. Pomelli, J. W. Ochterski, R. L. Martin, K. Morokuma, V. G. Zakrzewski, G. A. Voth, P. Salvador, J. J. Dannenberg, S. Dapprich, A. D. Daniels, O. Farkas, J. B. Foresman, J. V. Ortiz, J. Cioslowski, and D. J. Fox, Gaussian, Inc., Wallingford CT, 2013.
- [14] H. B. Schlegel, Optimization of equilibrium geometries and transition structures, *J. Comput. Chem.*, **1982**, 3, 214–218.
- [15] Silverstein, R. M., Bassler, G. C., Morrill, T. C. (1991) *Spectrometric Identification of Organic Compounds*, John Wiley, Chichester.
- [16] Socrates, G. (2001) *Infrared and Raman Characteristic Group Frequencies—Tables and Charts*, third ed., Wiley, New York.
- [17] A. N. Prabhu, A. Jayarama, K. Subrahmanya Bhat, V. Upadhyaya, *J. Mol. Struct.* 1031, 79 (2013).
- [18] G. Keresztury, in: *Handbook of Vibrational Spectroscopy*, Eds. J. M. Chalmers, P. R. Gri-ths, Vol. 1, Wiley, New York 2002.
- [19] G. Varsanyi, *Assignments of Vibrational Spectra of 700 Benzene Derivatives*, Wiley, New York 1974.
- [20] C. Sridevi, G. Velraj, *Spectrochim. Acta A* 107, 334 (2013).
- [21] J. Zinczuk, A. E. Ledasma, S. A. Brandan, O. E. Piro, J. J. L. Gonzalez, A. B. Atabef, Structural and vibrational study of 2-(2'-furyl)-4,5-1 H-dihydroimidazole, *J. Phys. Org. Chem.*, 2009, 22, 1166–1177.
- [22] N. Ramesh Babu et al., Synthesis and spectral characterization of hydrazone derivative of furfural using experimental and DFT methods, *Spectrochim Acta.*, 2014, 120, 314–322.
- [23] H. Alyar, Z. Kantarci, M. Bahat, E. Kasap, Investigation of torsional barriers and nonlinear optical (NLO) properties of phenyltriazines, *J. Mol. Struct.*, 2007, 834, 516–520.
- [24] Scrocco E, Tomasi J. Electronic molecular structure, reactivity and intermolecular forces: an heuristic interpretation by means of electrostatic molecular potentials. *Adv Quantum Chem.* 1978;11:115.
- [25] R. G. Parr, W. Yang, *J. Am. Chem. Soc.* 106 (1984) 4049–4050.